Urol Res (1991) 19:381–385

Urological Research

High-speed photographic evaluation of endoscopic lithotripsy devices

H. J. C. M. Sterenborg[1], Th. M. de Reijke[2], J. Wiersma[1], R. C. Erckens[1], and F. H. M. Jogsma[3]

[1]Laser Centre and [2]Department of Urology, Academic Hospital of the University of Amsterdam, Amsterdam, The Netherlands
[3]Department of Ophthalmology, University of Limburg, Maastricht, The Netherlands

Accepted: March 1, 1991

Summary. Shock-wave generation and bubble formation occurring during endoscopic lithotripsy were studied using high-speed photography for various devices: a pulsed-dye laser, a Q-switched Nd:YAG laser and an electrohydraulic (EHL) apparatus. The three devices investigated generated gas bubbles that rapidly expanded and decayed. The maximal size of these bubbles was 5–8 mm for the pulsed-dye laser, 6 mm for the Q-switched Nd:YAG laser and up to 14 mm for the EHL device. The bubble size appeared to be governed mainly by the energy per pulse delivered by the lithotripsy device. The shock-wave pattern depended strongly on the type of device used; the 25-ns Q-switched Nd:YAG laser pulse generated a single pressure step, whereas the 1.5-μs pulsed-dye laser produced a train of shock fronts.

Key words: High-speed photography – Shock wave – Electrohydraulic lithotripsy – Laser lithotripsy – Stone fragmentation

In recent years, the treatment of stones in the urinary tract has changed from an open surgical procedure into an endourological intervention; since 1980, extracorporeal shockwave-lithotripsy (ESWL) has been used [1]. For 3 years, ESWL has also been the preferred treatment modality for stones in the ureter. The rates of success for this therapy vary between 41% and 97% [7]. If stones have been impacted or have remained in situ for >8 weeks, the success rate drops significantly. In this case, multiple ESWL sessions are usually needed or alternative procedures for stone removal are indicated [4].

One alternative modality is ureteroscopy. By this route the impacted stone can be disintegrated under direct vision using ultrasonic lithotripsy, electrohydraulic lithotripsy (EHL) or laser lithotripsy. Ultrasonic lithotripsy has the advantage that all the fragments can be removed by suction. For this method, however, large-caliber ureteroscopes (11 F) are needed. Pressure is required for hard stones, inducing the risk of pushing the stone through the ureteral wall [10]. Various studies have shown that ureteric damage (perforation, stricture formation) occurs mainly as a result of the instrumentation used [16]. On the basis of this knowledge, disintegration systems were studied that enable the application of small-caliber and flexible instruments, providing safe and adequate disintegration. The two modalities available for this purpose are EHL and laser lithotripsy.

The EHL probe can be placed near the stone through thin instruments or flexible ureteroscopes. The device generates a shock wave by inducing a short electric discharge at the tip of the catheter. The energy released in the discharge is relatively high usually amounting to 1–3 J. At such high levels of energy, occasional negative side effects have been observed:

1. Rupture of the ureteral wall or penetration of the wall of the ureter by fragments; when the stone is impacted in the wall, there is a particularly high probability of ureteric damage.
2. The electrical insulation on the tip of the catheter may be damaged, directly exposing the ureteral wall to the spark.
3. The production of heat, the avoidance of which requires thorough water irrigation [5, 8, 18].

Laser lithotripsy can be performed through a flexible uterescope. The energy is passed through an optical fiber measuring 300–600 μm in diameter. The fiber is placed directly on the stone. Light pulses releasing levels of energy of between 25 and 100 mJ are applied to the stone and generate shock waves that fragment it. At pulse-repetition rates of ≤ 10 Hz, no thermal injury to the ureter can occur. Teng et al. [12] have reported the generation of cavitation bubbles on the surface of a kidney stone immediately following the laser pulse. A mathematical model was developed by Lo et al. [6] that predicts the bubble radius and pressure as functions of time.

The aim of the present investigation was to evaluate and compare the shock-wave patterns and bubbles generated by different lithotripsy devices in clinical use.

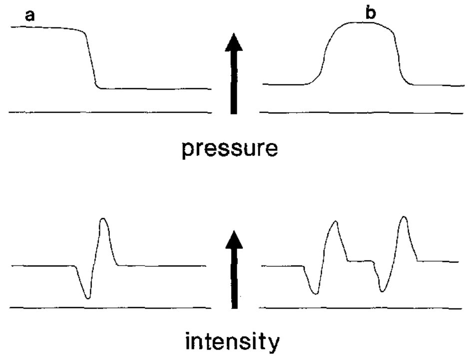

Fig. 1 a, b. Shock-wave pressure shape and associated light pattern for **a** single step in pressure and **b** a pressure peak or double step in pressure

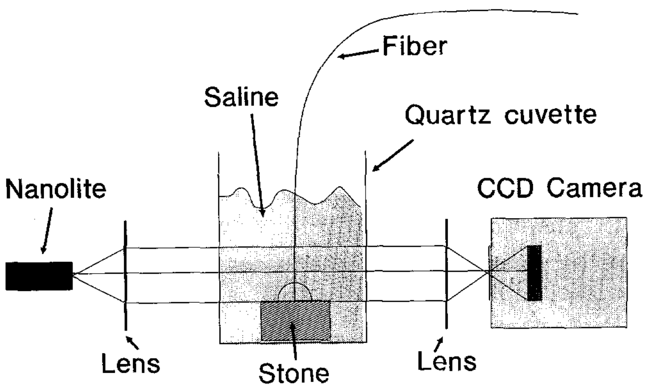

Fig. 2. The practical outlines of the experimental setup

Materials and methods

Photography

Shock waves travel in water at a velocity at least equalling that of sound, i.e. 1,500 m/s. To record such a high-speed phenomenon photographically, a sub-micro-second exposure time is necessary. In our experiments we used a specially designed flashlamp (Nanolite) at a flash duration of 0.02 µs. A standard charge-coupled device (CCD) camera was used to record the images.

Fig. 3a–c. Images taken using the pulsed-dye laser at 28 mJ/pulse and at intervals of **a** 5 µs, **b** 250 µs and **c** 550 µs

The photographic technique used to image the shock waves is based on variations in the index of refraction. Pressure gradients in a shock wave can be quite high. This pressure gradient and the associated gradients in the density and, cosequently, in the index of refraction of the medium are sufficiently large to deflect a light beam. When a parallel and homogeneous light beam passes the shock-wave region, the variations in the intensity occurring the image plane are proportional to the second time derivative of the pressure [17]. Hence, a single step in pressure induces an intense light band followed by a dark band (Fig. 1a), whereas a pressure impulse (up and down again) or a double step is expressed as twice the above-mentioned pattern (Fig. 1b). Air bubbles in water act as negative lenses; they are recorded by the light deflections at their boundaries.

The practical outlines of the setup are shown in Fig. 2. The shock-wave-generating part of the lithotripsy device under investigation is placed in water to obtain an acoustic match of the in vivo situation. Once the device has been fired, an electronic delay unit is triggered, which discharges the Nanolite after a predefined delay time. This delay time can be varied in the range of 0.1 µs to 10 ms. The images taken by the CCD camera are stored on a standard video cassette recorder and, after selection, are printed by a video printer.

Lithotripsy devices

The devices investigated included the Wolf Riwolith, EHL system; the MBB Litholas, a Q-switched Nd:YAG laser using a 600-µm fiber with a sideward-directed metal tip; and the Candela LFDL/3 equipped pulsed-dye laser with a 600-µm core fiber. The first two devices generate shock waves independently of the availability of a stone, whereas the pulsed-dye laser does not. Only after the laser pulse from this device has hit the surface of a stone is a shock wave generated. In the present experiment we used a black-coated sheet of aluminum to simulate a stone.

Results

Images recorded following application of the pulsed-dye laser are shown in Fig. 3. The concentric circles in Fig. 3a represent a series of shock waves travelling through the water. Obviously, shock waves in the "stone" can not be visualized in this way. Figures 3a and 3b illustrate the images taken at 100 and 250 µs after the laser pulsed, respectively, showing a hemispherical bubble on the surface of the stone. After 550 µs (Fig. 3c), "long" after the laser pulse, another shock wave was formed as a result of the implosion of the bubble [13].

The growth of the bubble as a function of time was measured by taking two series of pictures at various delay times. The bubble diameters were measured and are

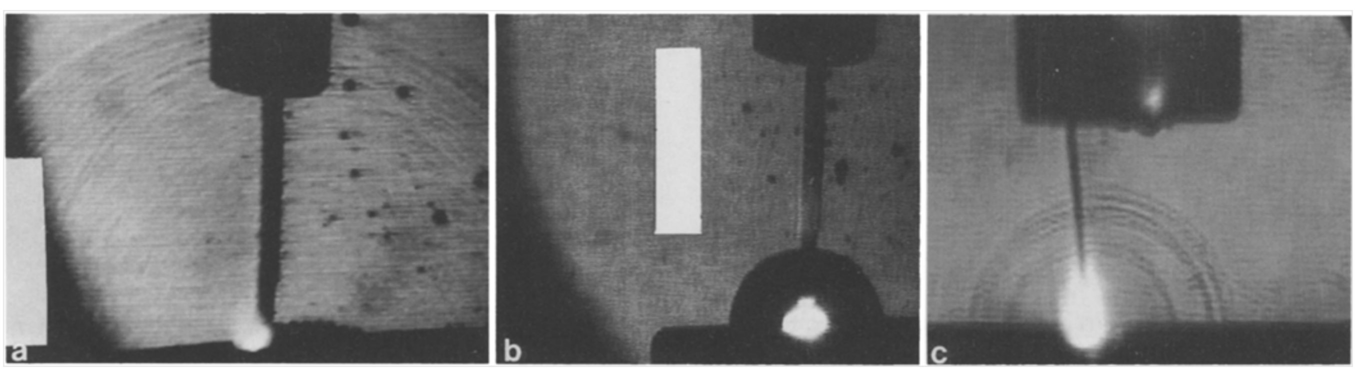

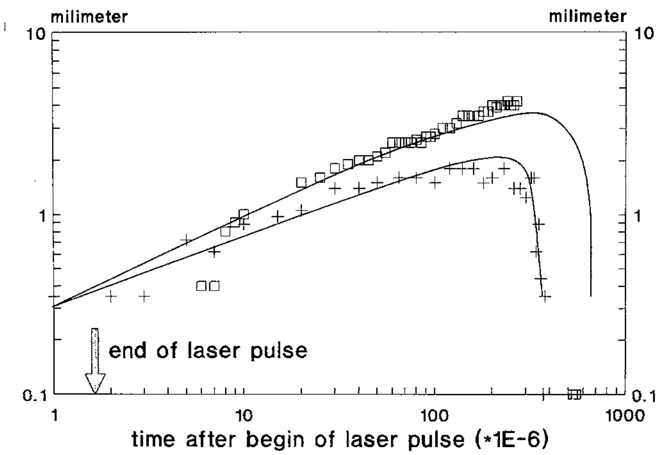

Fig. 4. The size of a hemispherical bubble created with the pulsed-dye laser on black-painted aluminum as a function of time. The fiber diameter was 600 μm. The *line* was drawn according to the model of Lo et al. [6]. +, 30 mJ; □, 60 mJ

depicted in Fig. 4. The points closely follow the shape of the curve predicted by the mathematical model developed by Lo et al. [6].

Images obtained using the MBB Litholas are shown in Figs. 5a and 5b (3 and 200 μs, respectively). The shock wave generated is visible as a circular segment directed slightly upwards. In contrast to Fig. 3a, Fig. 5 demonstrates a single pressure step. The irregular disturbances in the bottom half of the image are caused by flushing liquid emerging from the tip of the device. These do not represent shock waves but are caused by small differences in the index of refraction between the flushing liquid and the bulk liquid in the cuvette. Figure 5b shows a small bubble emerging from the hole in the laser catheter. The maximal bubble size (3–4 mm) at 40 mJ/pulse is shown in Fig. 5b.

The images obtained using the Wolf Riwolith EHL probe are shown in Fig. 6. In Fig. 6a, a series of shock waves are apparent. Figure 6b shows the maximal bubble size attained with this device. The exact delay time is not known, as frequent mistriggering of the delay unit occurred due to the electric disturbances generated by the electric discharge in the EHL probe. The diameter of the bubble shown in Fig. 6b was estimated to be 14 mm. The

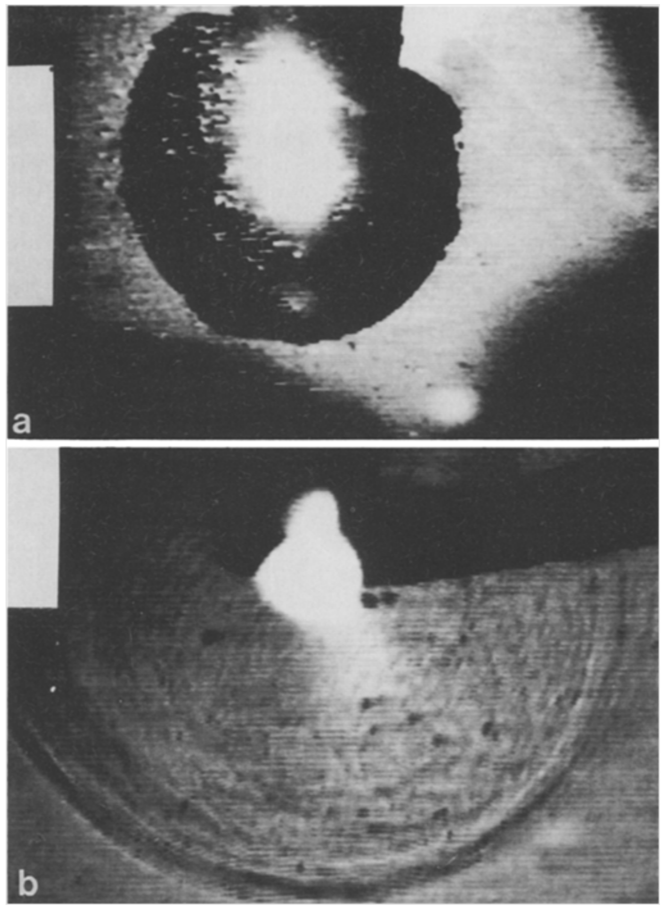

Fig. 6a, b. Images taken using the Wolf Riwolith at 1 J/pulse. **a** Shock-wave pattern. **b** Maximal bubble size

electric energy of the discharge was estimated to be in the range of 1–3 J.

Discussion

Shock-wave patterns

The shock waves generated using the pulsed-dye laser (Fig. 3a) and the EHL device (Fig. 6a) were visualized as a large number of light and dark bands, indicating the

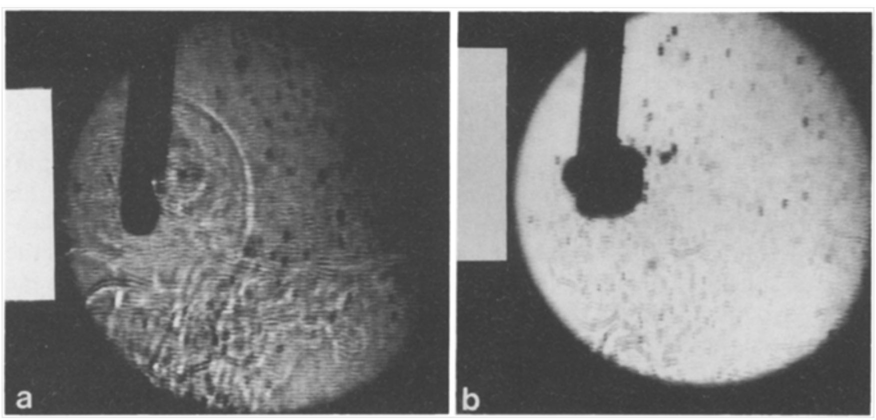

Fig. 5a, b. Images taken using the MBB Litholas at 40 mJ/ pulse and at delay times of **a** 3 μs and **b** ±200 μs (maximal size)

Table 1. Comparison of the different endoscopic disintegration systems available for ureteral stones

	Pulsed-dye laser	MBB Litholas	Electrohydraulic	Ultrasound
Diameter	600 µm	1.2 mm	0.9 mm	1.8 mm
Instrument	Flexible	Flexible	Flexible	Rigid
Vision	Endoscope	Fluoroscope, endoscope	Endoscope	Endoscope
Damage	(Perforation)	Minimal	Bubble	Pressure
Cost	Expensive	Expensive	Inexpensive	Inexpensive
Size of equipment	$\pm 1\ m^3$	$\pm 0.1\ m^3$	Small	Small

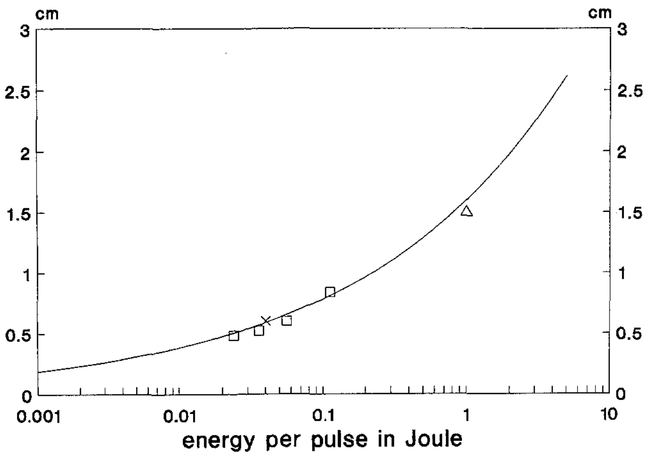

Fig. 7. The maximal bubble diameter as a function of the energy used per pulse. The *line* was drawn according to the mathematical model by Lo et al. [6]. □, Pulsed-dye laser; ×, MBB Litholas; △, EHL

occurrence of multiple shock fronts. The delay times used to obtain two images reveal that shock-wave generation continued throughout the driving (laser or electrical) pulse (± 1 µs). In the case of the Q-switched Nd:YAG laser, the pulse was much sorter (25 ns), which resulted in a single stepwise change in pressure.

Maximal bubble size

The maximal sizes of the bubbles generated by the three devices are shown in Fig. 7. The measurements obtained closely matched the shape of the curve generated by the mathematical model described by Lo et al. [6]. This suggests that once the bubble has been produced, its behaviour is independent of the mechanism by which it is generated.

Damage to the ureter

When EHL probes are used in the ureter, occasional ureteric rupture may occur. This may be attributable to the action of the expanding bubble. Although the spherical shape of the bubble may be disturbed in vivo, the expansive force exerted on the ureter may well exceed the limits for reversible elastic deformation, resulting in instantaneous damage to the ureteral wall. Also, less destructive bubbles may irritate the ureteral wall and give rise to local edema or other delayed reactions. Moreover, the rapidly expanding bubble may push stone fragments into or through the ureteral wall. When lasers are used at levels of energy within the range of 30–60 mJ/pulse, such acute or delayed reactions are not observed [2]. This suggests that the complication rate following endoscopic lithotripsy using EHL devices could be lowered by decreasing the amount of energy applied per pulse. Whether the resultant fragmentation capacity would be adequate cannot be determined on the basis of the present analysis.

Stone propulsion

The large size of the bubbles generated at higher levels of pulse energy may have another consequence. The expanding bubble pushes not only against the ureteral wall but also against the stone. This may cause propulsion of the stone. Watson [15] has reported stones' being blasted from the ureter into the kidney following the application of a pulsed-dye laser at levels of energy ranging from 100 to 140 mJ/pulse. In in vitro experiments using various types of lasers at 1-8 J/pulse, similar propulsion phenomena have been observed [14].

Clinical consequences

For the treatment of ureteral calculi, extracorporeal shock-wave lithotripsy (ESWL) is the first option. In case this fails, ureteroscopic disintegration is an alternative approach. However, ureterorenoscopy demands experience, and even under the best circumstances, a 4%–10% chance of ureteric damage remains when a rigid instrument is use [3, 11]. Thin, flexible instruments are favoured for this technique. Besides the hazards of the instrumentational procedure, the disintegration process can also damage as a side effect. When the dye laser is used, mistargeting of the fiber may cause a small (600 µm) perforation in the ureteral wall. In clinical practice this occurs only rarely and has no important clinical implications. However, such damage cannot be inflicted when the MBB Litholas is applied because of the metal cap at the end of the fiber. The rapidly expanding bubbles investigated in the present study may also damage the ureteral wall; bubbles larger than the ureteral lumen might push stone fragments through the wall or even rupture the ureter itself. From our study it is evident that the 15-mm bubbles generated by the EHL device may represent a serious hazard to the ureteral wall.

Conclusions

The three endoscopic lithotripsy devices investigated produce a shock wave but also generate a rapidly expanding and quickly imploding gas bubble. For the pulsed-dye laser, the growth of this bubble closely follows the mathematical model described by Lo et al. [6]. The maximal bubble size matched this model for all devices studied. The MBB Litholas generated a single, slightly backward-directed shock front, whereas both the pulsed-dye laser and the EHL device generated multiple shock waves. For both of the lasers the maximal bubble size ranged from 5 to 7 mm, whereas the EHL device produced bubbles measuring up to 14 mm in maximal size.

Considering these observations, the laser seems to be the safest solution when ESWL failed. However, the negative aspects of laser lithotripsy include the high cost and the large size of the equipment and the necessity for special safety procedures. Hopefully, these secondary disadvantages will be eliminated in the near future.

Acknowledgements. The authors would like to thank Mr. A. P. J. Wijnands of the Physics Department of the Technical University of Eindhoven for the providing access to the Nanolite flashlamp and Mr. P. Sterrenburg of Stöpler b.v. as well as Mr. H. Hirschke of MBB-Medizintechnik GmbH for enabling us to use the MBB Litholas.

References

1. Chaussy CG, Schmiedt E (1982) Shockwave treatment for stones in the upper urinary tract. Urol Clin Am 10:743
2. Coptcoat MJ, Ison KT, Watson G, Wickham JEA (1988) Lasertripsy for ureteric stones in 120 cases: lessons learned. Br J Urol 61:487–489
3. Dretler SP (1990) Ureteral stone disease: options for management. Urol Clin North Am 17:217–230
4. Goodfriend R (1984) Ultrasonic and electrohydraulic lithotripsy of ureteral calculi. Urology 23:5
5. Green DF, Lytton B (1985) Early experience with direct vision electrohydraulic lithotripsy of ureteral calculi. J Urol 23:767
6. Lo EY, Petschek H, Rosen DI (1990) A hydrodynamic model for the laser-induced fragmentation of calculi. Lasers Life Sci (in press)
7. Muller SC, Wilbert D, Thuroff JU (1986) Extracorporeal shockwave lthotripsy of ureteral stones: clinical experience and experimental findings. J Urol 25:831
8. Raney A (1978) Electrohydraulic lithotripsy. Urology 12:284
9. Reuter HJ, Kern E (1973) Electrohydraulic lithotripsy of ureteral calculi. J Urol 110:181
10. Schmiedt E, Chaussy CG (1984) Extracorporeal shochkwave lithotripsy of kidney and ureteral stones. Urol Int 39:193
11. Sosa RE, Vaughan ED Jr (1988) Complication of ureteroscopy. Am Urol Assoc Update 35:7
12. Teng P, Nishioka N, Anderson R, Deutsch T (1987) Acoustic studies of the role of immersion in plasma-mediated laser ablation. IEEE J Quantum Electron 23:1845
13. Vogel A, Lauterborn W, Timm R (1989) Optical and acoustical investigations of the dynamics of laser-produced cavitation bubbles near a solid boundary. J Fluid Mech 206:299–338
14. Watson G (1988) A survey of the action of lasers on stones. In: Steiner R (ed) Laser lithotripsy. Springer, Berlin Heidelberg New York, pp 15–24
15. Watson G (1989) First International Workshop and Symposium on new Urological technologies. Leuven, Belgium, September 1989.
16. Watson G, Murray S, Dettler S, Parrish JA (1987) An assessment of the pulsed dye laser for fragmenting calculi in the pig ureter. J Urol 138:199
17. Wen-Jei, Yi Cheng (1989) Optical methods in flow visualization. J Laser Appl 1:31–39
18. Willscher MK, Conway JF, Babyan RK et al. (1988) Safety and efficacy of electrohydraulic lithotripsy by ureteroscopy. J Urol 140:957

H. J. C. M. Sterenborg, MD
Laser Center
Academic Hospital
University of Amsterdam
Meibergdreef 9
1105 AZ Amsterdam
The Netherlands